Available online at www.sciencedirect.com
ScienceDirect
Ceramics International 37 (2011) 679–682
CERAMICS INTERNATIONAL
www.elsevier.com/locate/ceramint

Short communication

Rapid consolidation of nanostructured $TaSi_2$ from mechanochemically synthesized powder by high frequency induction heated sintering

In-Jin Shon [a,b,*], In-Yong Ko [a], Seung-Myoung Chae [a], Kwon-il Na [a]

[a] Division of Advanced Materials Engineering, The Research Center of Advanced Materials Development, Chonbuk National University, 664-14 Deokjin-dong 1-ga, Deokjin-gu, Jeonju, Jeonbuk 561-756, Republic of Korea
[b] Department of Hydrogen and Fuel Cells Engineering, Specialized Graduate School, Chonbuk National University, 664-14 Deokjin-dong 1-ga, Deokjin-gu, Jeonju, Jeonbuk 561-756, Republic of Korea

Received 4 January 2010; received in revised form 10 August 2010; accepted 24 September 2010
Available online 29 October 2010

Abstract

Nanopowder of $TaSi_2$ was synthesized from Ta and 2Si during high energy ball milling for 20 h. Dense nanostructured $TaSi_2$ was consolidated by high frequency induction heated sintering method within 2 min from mechanically activated powders of $TaSi_2$. Highly dense $TaSi_2$ with relative density of up to 98% was produced under simultaneous application of a 80 MPa pressure and the induced current. The average grain size and hardness of the compound were investigated.

Keywords: Rapid sintering; Intermetallic; Nanophase; $TaSi_2$; Mechanical properties

1. Introduction

An increase in operating temperature of a gas turbine engine will bring us reductions in both fuel consumption and CO_2 emissions. It requires ultra-high temperature structural materials which overwhelm the performance of nickel-based superalloys commercially used as turbine blade and rotors. In this regard, transition-metal silicides are very attractive for application temperature up to 1300 °C and higher because this class of materials has an attractive combination of properties, including high melting temperature, high modulus, high oxidation resistance in air, and a relatively low density [1,2]. In addition, the thermal and electrical conductivities are relatively high and therefore they are also attractive for electronic interconnections and diffusion barriers. Most of the investigations on silicides have focused on a few compounds, with $MoSi_2$ and $TiSi_2$ being the most studied. Other silicides, such as $TaSi_2$, WSi_2, $NbSi_2$, $ZrSi_2$ and VSi_2 have received relatively little attention. The melting point, crystal structure, density, formation enthalpy at 298 K, and adiabatic temperature of $TaSi_2$ are 2025 °C, hexagonal, 9.205 g/cm^3, 32.4 KJ mol^{-1}, and 1795 K [3–5].

As in the case of many intermetallic compounds, the current concern about these materials focuses on their low fracture toughness below the ductile-brittle transition temperature [6,7]. To improve on their mechanical properties, the approach commonly utilized has been the addition of a second phase to form composites and nanostructured materials [8–13].

Nanostructured materials have been widely investigated because they display a wide functional diversity and exhibit enhanced or different properties compared with bulk materials [14]. Particularly, in the case of nanostructured ceramics, the presence of a large fraction of grain boundaries can lead to unusual or better mechanical, electrical, optical, sensing, magnetic, and biomedical properties [15–20]. In recent days, nanocrystalline powders have been developed by co-pricipitation, the thermochemical and thermomechanical process named as the spray conversion process (SCP) and high energy milling [21,22]. However, the grain size in sintered materials becomes much larger than that in pre-sintered powders due to a fast grain growth during conventional sintering process. Therefore, even though the initial particle size is less than 100 nm, the grain size increases rapidly up to 500 nm or larger during the conventional sintering [23]. So, controlling grain growth during sintering is one of the keys to the commercial

* Corresponding author at: Division of Advanced Materials Engineering, The Research Center of Advanced Materials Development, Chonbuk National University, 664-14 Deokjin-dong 1-ga, Deokjin-gu, Jeonju, Jeonbuk 561-756, Republic of Korea. Tel.: +82 63 2381; fax: +82 63 270 2386.
E-mail address: ijshon@chonbuk.ac.kr (I.-J. Shon).

0272-8842/$36.00
doi:10.1016/j.ceramint.2010.09.054

success of nanostructured materials. In this regard, the high frequency induction heated sintering method which can make dense materials within 2 min, has been shown to be effective in achieving this goal [24,25].

The objective of this study is to make nanopowder by high energy ball milling and to investigate the preparation of dense nanophase $TaSi_2$ by the HFIHS method starting from mechanically synthesized powders.

2. Experimental procedure

Powders of 99.97% pure tantalum (−325 mesh, Alfa Products, Ward Hill, MA) and 99% pure silicon (−325 mesh, Aldrich Products, Milwaukee, WI) were used as starting materials. Powder mixtures of Ta and Si in the molar proportion of 1:2 were first milled in a high-energy ball mill (Pulverisette-5, planetary mill) at 250 rpm for 20 h. Tungsten carbide balls (5 mm in diameter) were used in a sealed cylindrical stainless steel vial under argon atmosphere. The weight ratio of ball-to-powder was 30:1. The grain size and the internal strain were calculated by Suryanarayana and Grant Norton's formula [26],

$$B_r\,(B_{crystalline} + B_{strain})\cos\theta = \frac{k\lambda}{L} + \eta\sin\theta \quad (1)$$

where B_r is the full width at half-maximum (FWHM) of the diffraction peak after instrument correction; $B_{crystalline}$ and B_{strain} are FWHM caused by small grain size and internal stress, respectively; k is constant (with a value of 0.9); λ is wavelength of the X-ray radiation; L and η are grain size and internal stress, respectively; and θ is the Bragg angle. The parameters B and B_r follow Cauchy's form with the relationship: $B = B_r + B_s$, where B and B_s are FWHM of the broadened Bragg peaks and the standard sample's Bragg peaks, respectively. After milling, the powders were placed in a graphite die (outside diameter, 45 mm; inside diameter, 20 mm; height, 40 mm) and then introduced into the high frequency induction heated sintering system made by Eltek Co. in Republic of Korea presented in Ref. [24,25]. The system was first evacuated and a uniaxial pressure of 80 MPa was applied. The HFIHS apparatus includes an 15 kW power supply (which provides a frequency of 50 kHz) and a 50 kN uniaxial press. A induced current was then activated and maintained until the densification rate was negligible, as indicating by the observed shrinkage of the sample. Sample shrinkage is measured in real time by a linear gauge measuring the vertical displacement. Temperatures were measured by a pyrometer focused on the surface of the graphite die. The heating rates were approximately 1000 °C/min in the process. At the end of the process, the induced current was turned off and the sample was allowed to cool to room temperature. The entire process of densification using the HFIHS technique consists of four major control stages. These are chamber evacuation, pressure application, power application, and cool down. The process was carried out under a vacuum of 40 mTorr.

The relative densities of the synthesized sample were measured by the Archimedes method. Microstructural characterization was made on product samples which had been polished and etched using a solution of HF (30 vol.%), HNO_3 (30 vol.%) and H_2O (40 vol.%) for 7 s at room temperature. Compositional and microstructural analyses of the products were made through X-ray diffraction (XRD) and scanning electron microscopy (SEM) with energy dispersive X-ray analysis (EDAX). Vickers hardness was measured by performing indentations at a load of 10 kg and a dwell time of 15 s.

3. Results and discussion

Fig. 1 shows XRD patterns of powder milled for 10, 20 h and $TaSi_2$ sintered from milled powder for 20 h. In Fig. 1(a), reactants of Ta and Si peaks are detected but in Fig. 1(b), $TaSi_2$ is synthesized during milling for 20 h. The interaction between these phases (Ta and Si), i.e.,

$$Ta + 2Si \rightarrow TaSi_2, \quad (2)$$

is thermodynamically feasible.

The average grain size of the synthesized $TaSi_2$ and the sintered $TaSi_2$ calculated by the C. Suryanarayana and M. Grant Norton's formula [26] were about 23 nm and 60 nm,

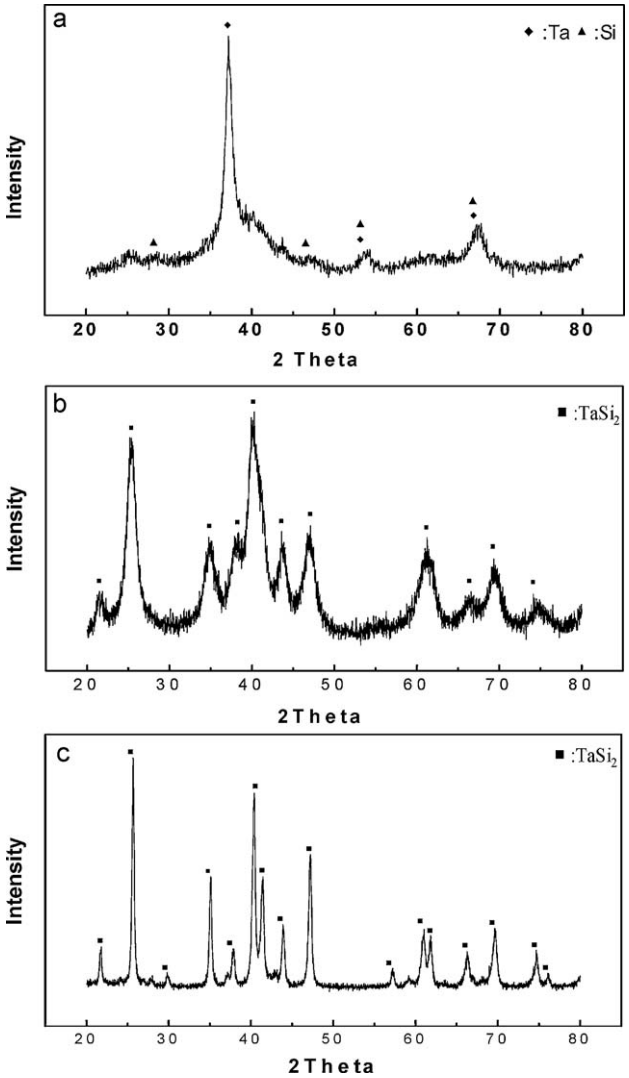

Fig. 1. XRD patterns of milled Ta + 2Si powder for (a) 10 h, (b) 20 h and (c) $TaSi_2$ sintered from mechanochemically synthesized $TaSi_2$.

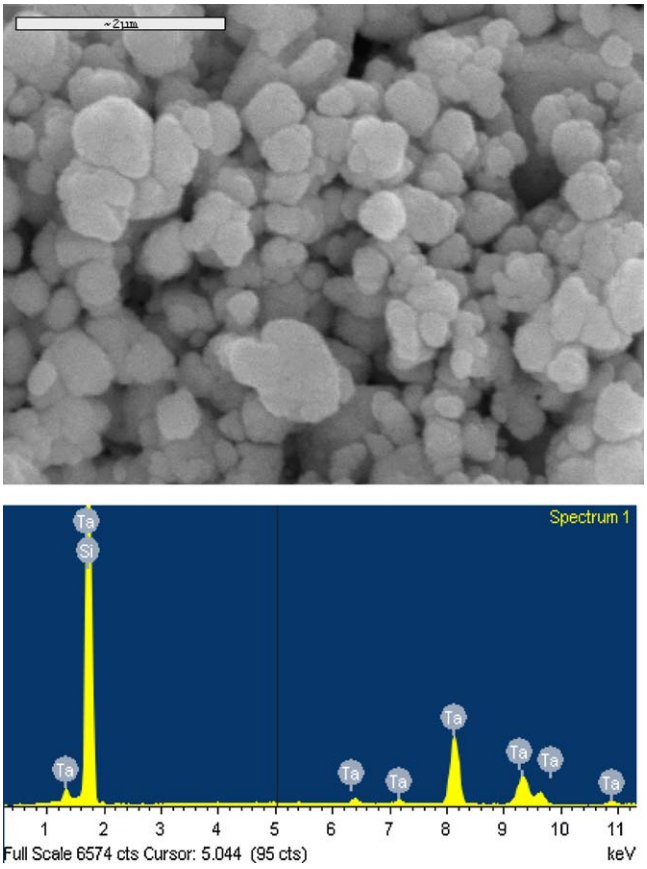

Fig. 2. FE-SEM image and EDS analysis of $TaSi_2$ powder milled for 20 h.

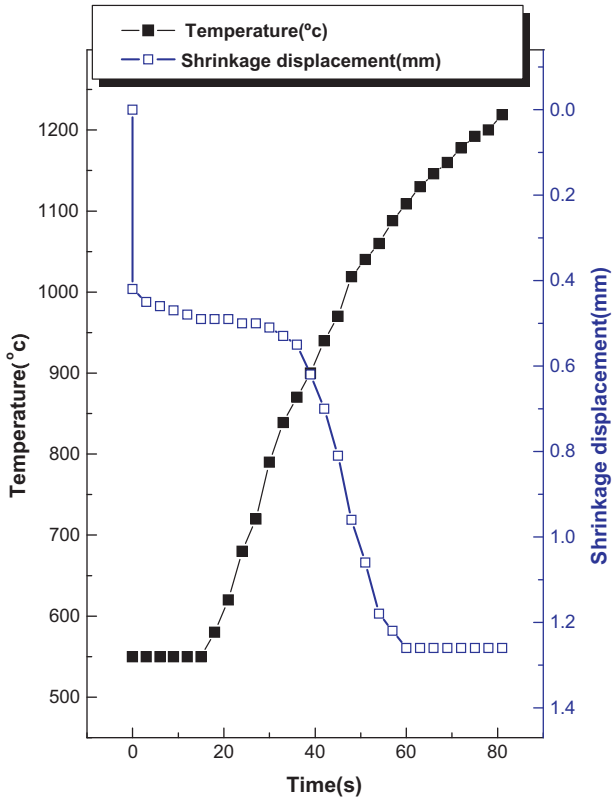

Fig. 3. Variations of temperature and shrinkage displacement with heating time during high frequency induction heated densification of $TaSi_2$.

respectively. Plot of $B_r \sin\theta$ versus $\cos\theta$, Th intercept ($k\lambda/L$) from plot of $B_r \sin\theta$ versus $\cos\theta$ can be used to calculate the crystallite size (L).

Fig. 2 shows FE-SEM image and EDS analysis of powder milled for 20 h. The particle of $TaSi_2$ has nanograin and heavier contamination such as WC from milling balls and iron from a milling container were not detected in EDS. The variations in shrinkage displacement and temperature with heating time during the processing of $TaSi_2$ are shown Fig. 3. As the induced current was applied to reacted powder of $TaSi_2$ the shrinkage

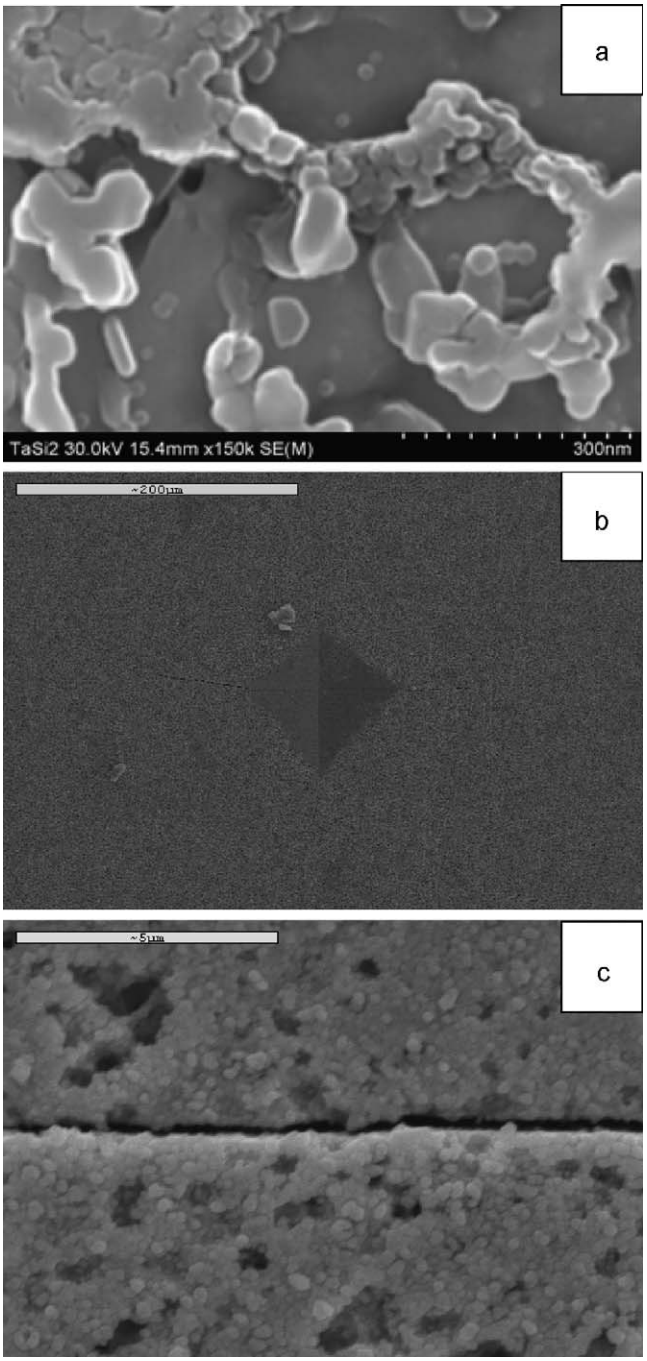

Fig. 4. (a) FE-SEM image of $TaSi_2$ sintered from mechanochemically synthesized $TaSi_2$, (b) Vickers hardness indentation and (c) median crack propagating in $TaSi_2$.

displacement gradually increased up to 850 °C and then abruptly increased. XRD pattern of $TaSi_2$ sintered at 1220 °C is shown in Fig. 1(c). Only $TaSi_2$ peaks are detected. Fig. 4 shows microstructure, Vickers hardness indentation and median crack propagating in $TaSi_2$ sintered from mechanically synthesized $TaSi_2$. $TaSi_2$ consists of nanograin in Fig. 4(a). Vickers hardness measurements were made on polished sections of the $TaSi_2$ using a 10 kg load and 15 s dwell time. The calculated hardness value, based on an average of five measurements, of the $TaSi_2$ is 13 GPa. In Fig. 4(b) cracks produce around the indent and the crack propagates linearly in Fig. 4(c). The absence of reported values for hardness on $TaSi_2$ precludes making direct comparison to the results obtained in this study to show the influence of grain size.

4. Summary

Using the high frequency induction heated sintering method, the densification of nanostructured $TaSi_2$ was accomplished from powders of mechanochemically synthesized $TaSi_2$. Complete densification can be achieved within 2 min. The relative density of the composite was 98% under an applied pressure of 80 MPa and the induced current. The average grain sizes and hardness of $TaSi_2$ phases were about 60 nm and 13 GPa, respectively.

Acknowledgement

This work was supported by the Korea Research Foundation (KRF) Grant funded by the Korean Government (MEST) (KRF-2009-0065776).

References

[1] A.K. Vasudevan, J.J. Petrovic, J. Mater, ZrO_2 and ZrO_2 – SiC particle reinforced $MoSi_2$ matrix composites, Sci. Eng. A 155 (1992) 259–266.
[2] G.J. Fan, M.X. Quan, Z.Q. Hu, J. Eckert, L. Schulz, In-situ explosive formation of $NbSi_2$-based nanocomposites by mechanical alloying, Scr. Mater. 41 (1999) 1147–1151.
[3] H. Okamoto, Phase diagrams for binary alloys, ASM International, 2000, p. 735.
[4] O. Knacke, O. Kubaschewski, K. Hesselmann, Thermochemical Properties of Inorganic Substances, Springer-Verlag, 1973, 1991.
[5] F. Chu, M. Lei, S.A. Maloy, J.J. Petrovic, T.E. Mitchell, Elastic properties of C40 transition metal disilicides, Acta Mater. Acta Mater. 44 (1966) 3035–3048.
[6] G. Sauthoff, Intermetallics, VCH Publishers, New York, 1995.
[7] Y. Ohya, M.J. Hoffmann, G. Petzow, Mechanical properties of hot-pressed SiC–TiB_2/TiC composites synthesized in situ, J. Mater. Sci. Lett. 12 (1993) 149–155.
[8] B.W. Lin, T. Iseki, Effect of thermal residual stress on mechanical properties of SiC/TiC composites, Br. Ceram. Trans. J. 91 (1992) 1–6.
[9] Y. Ohya, M.J. Hoffmann, G. Petzow, Sintering of in-situ synthesized SiC–TiB_2 composites with improved fracture toughness, J. Am. Ceram. Soc. 75 (1992) 2479–2483.
[10] S.K. Bhaumik, C. Divakar, A.K. Singh, G.S. Upadhyaya, Synthesis and sintering of TiB_2 and TiB_2–TiC composite under high pressure, J. Mater. Sci. Eng. A 279 (2000) 275–281.
[11] D.K. Jang, R. Abbaschian, A study of synthesis of (Mo, W)Si_2 composites, Korean J. Mater. Res. 9 (1999) 92–98.
[12] H. Zhang, P. Chen, M. Wang, X. Liu, Fractal dimension of profile of spherical wear debris and cutting wear debris, Rare Metals 21 (2002) 304–309.
[13] D.Y. Oh, H.C. Kim, J.K. Yoon, I.J. Shon, One step synthesis of dense $MoSi_2$–SiC composite by high-frequency induction heated combustion and its mechanical properties, J. Alloys Compd. 395 (2005) 174–179.
[14] H. Gleiter, Nanostructured material: state of the art and perspective, NanoStruct. Mater. 6 (1995) 3–14.
[15] J. Karch, R. Birringer, H. Gleiter, Ceramics ductile at low temperature, Nature 330 (1987) 556–558.
[16] H. Gleiter, Tuning the electronic structure of solids by means of nanometer-sized microstructures, Scripta mater. 44 (2001) 1161–1168.
[17] D. Hreniak, W. Strek, Synthesis and optical properties of Nd^{+3}-doped $Y_3Al_5O_{12}$ nanoceramics, J. Alloys Compd. 341 (2002) 183–186.
[18] C. Xu, J. Tamaki, N. Miura, N. Yamazoe, Grain size effects on gas sensitivity of porous SnO_2-based elements, Sens. Actuators B (3) (1991) 147–155.
[19] D.G. Lamas, A. Caneiro, D. Niebieskikwiat, R.D. Sanchez, D. Garcia, B. Alascio, Transport and magnetic properties of nanocrystalline $La_{2/3}Sr_{1/3}MnO_3$ powders synthesized by a nitrate–citrate gel-combustion process, J. Magn. Mater. 241 (2002) 207–213.
[20] E.S. Ahn, N.J. Gleason, A. Nakahira, J.Y. Ying, Nanostructure processing of hydroxyapatite-based bioceramics, Nano Lett. 1 (2001) 149–153.
[21] Z. Fang, J.W. Eason, Study of nanostructured WC–Co composites, Int. J. Refract. Met. Hard Mater. 13 (1995) 297–303.
[22] I.J. Shon, B.R. Kim, J.M. Doh, J.K. Yoon, Consolidation of binderless nanostructured titanium carbide by high-frequency induction heated sintering, Ceram. Int. 36 (2010) 1797–1803.
[23] M. Sommer, W.D. Schubert, E. Zobetz, P. Warbichler, On the formation of very large WC crystals during sintering of ultrafine WC–Co alloys, Int. J. Refract. Met. Hard Mater. 20 (2002) 41–50.
[24] H.C. Kim, I.J. Shon, J.K. Yoon, J.M. Doh, Comparison of sintering behavior and mechanical properties between WC−8Co and WC−8Ni hard materials produced by high-frequency induction heating sintering, Metals Mater. Int. 12 (2006) 141–147.
[25] H.C. Kim, I.J. Shon, I.K. Jeong, I.Y. Ko, Rapid sintering of nanocrystalline 8 mol.%Y_2O_3-stabilized ZrO_2 by high-frequency induction heating, Metals Mater. Int. 12 (2006) 393–398.
[26] C. Suryanarayana, M.G. Norton, X-ray Diffraction A Practical Approach, Plenum Press, New York, 1998.